Identification of tumorigenic cells and therapeutic targets in pancreatic neuroendocrine tumors

Geoffrey W. Krampitz[1,2,6], Benson M. George[2], Stephen B. Willingham[2], Jens-Peter Volkmer[2], Kipp A. Weiskopf[2], Nadine S. Jahchan[2,5], Aaron M. Newman[2], Debashis Sahoo[2], Allison Zemek[3], Rebecca L. Yanovsky[2], Julia K. Nguyen[2], Peter J. Schnorr[2], Pawel K. Mazur[2,5], Julien Sage[2,5], Teri A. Longacre[3], Jeffrey A. Norton[1,6], Irving L. Weissman[2,3,6]

[1]Department of Surgery, [2]Institute of Stem Cell Biology and Regenerative Medicine,[3]Department of Pathology, [4]Department of Oncology, [5]Department of Pediatrics and Genetics, [6]Ludwig Center for Cancer Stem Cell Biology and Medicine, Stanford University, Stanford, California

Introduction

Patients with pancreatic neuroendocrine tumors (PanNETs) have limited therapeutic options

Tumor initiating cells (TICs) are responsible for tumor development, metastasis, and recurrence

Targeting TICs is necessary to eradicate tumors

TICs remain uncharacterized in PanNETs

CD90 (cell surface antigen) and ALDHA1 (enzyme) are markers for TICs in other cancers

MET is principle regulator of PanNET aggressiveness in mouse models and cell lines

CD47 is a “don’t eat me” signal co-opted by cancers to evade innate immune surveillance

Methods & Materials

We performed an in-depth genomic, cell surface, and functional analysis of a PanNET tumor at different stages in the disease process from a single index patient. We then used 39 separate human tissue specimens (IRB Protocol 22185) to develop a novel PanNET cell line (APL1) and generate reproducible xenograft models. We profiled patient PanNET tumors using flow cytometry, immunostaining, RNASeq, gene-set enrichment analysis, proteomic profiling, and tissue microarray analysis to identify a tumorigenic population of cells and potential therapeutic targets. We used in vitro phagocytosis assays using BON and APL1 cells co-cultured with human donor or NOD scid gamma (NSG) mouse macrophages to screen potential immunotherapies. We used in vivo treatment experiments using NSG-xenograft or RIP-Cre Rb/p53/p130 mice to validate potential immunotherapies.

This project is funded by the Virginia and D. K. Ludwig Fund for Cancer Research, an Anonymous Donors Fund, the National Cancer Institute, Siebel Stem Cell Institute and the Thomas and Stacey Siebel Foundation, A. P. Giannini Foundation, American College of Surgeons, and Advanced Residency Training at Stanford, and SU2C-Lustgarten Foundation Pancreatic Cancer Convergence Dream Team.

Results

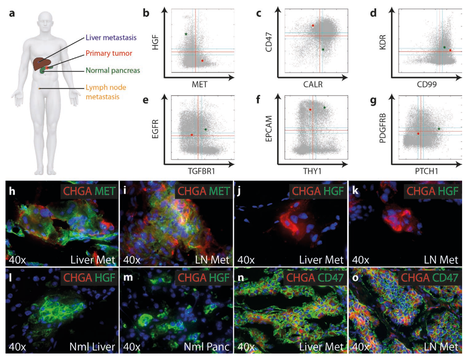

Figure 1. Profiling of an index patient’s PanNETs **(a)**. Gene expression analysis of the primary tumor and normal pancreas **(b-g)** shows aberrant expression of *HGF* and *MET* **(b)** and *CD47* **(c)**. Staining of CHGA and MET in the liver met **(h)** and LN met **(i)**. Staining of CHGA and HGF in the liver met **(j)** and LN met **(k)**. Staining of CHGA and HGF in normal liver **(l)** and pancreas **(m)**. Staining of CHGA and CD47 in the liver met **(n)** and lymph node met **(o)**.

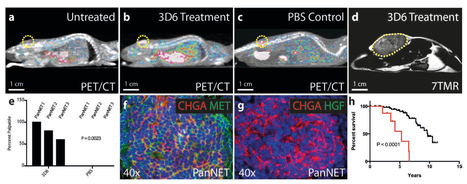

Figure 2. ^{18}F-FLT PET/CT of a dormant xenograft **(a)**, and after treatment with MET-agonist 3D6 (Genentech) **(b)** and control **(c)**. MRI of xenograft after 3D6 treatment **(d)**. 3D6 treatment increased engraftment efficiency compared to control **(e)**. Co-staining of CHGA and MET **(f)** but not CHGA and HGF **(g)**. High expression of MET decreases survival **(h)**.

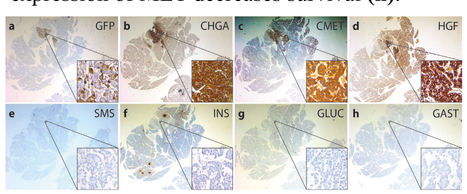

Figure 3. APL1 cell line engrafts into NSG mice **(a-b)**, express endogenous HGF and MET **(c-d)**, and are nonfunctional **(e-h)**.

Results

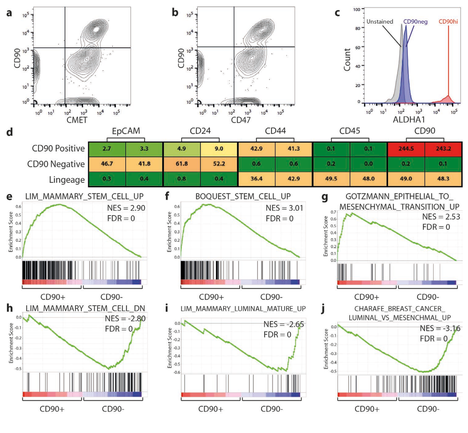

Figure 4. CD90 characterizes distinct cell populations by flow cytometry **(a-b)**. ALDHA1 activity is enhanced in CD90^{hi} vs. CD90^{neg} cells **(c)**. TIC markers are differentially expressed in CD90^{pos} and CD90^{neg} populations **(d)**. Gene set associated with stem cells are enriched in CD90^{hi} vs. CD90^{neg} cells **(e-j)**.

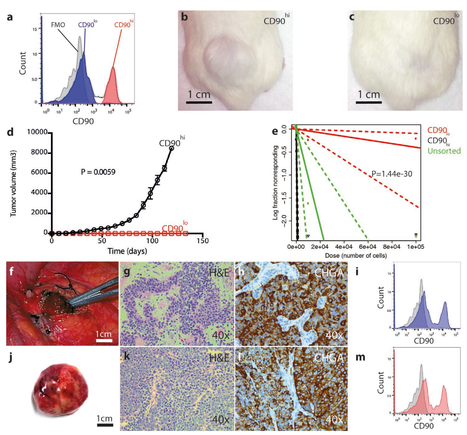

Figure 5. FACS-purified CD90^{hi} cells develop into tumors with high efficiency in NSG mice but CD90^{lo} cells do not **(a-c)**. CD90^{hi} and have sustained tumor growth but CD90^{lo} cells do not **(d)**. CD90^{hi} have increased tumorigenic potential compared to CD90^{lo} and unsorted cells **(e)**. Xenografts from CD90^{hi} cells recapitulate the features of the primary patient tumor **(f-m)**.

Results

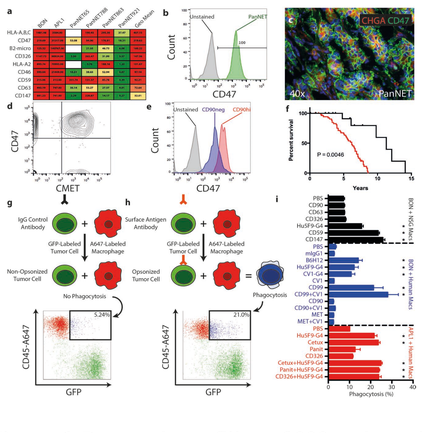

Figure 6. Proteomic profiling of 332 antigens in 2 cell lines and 4 primary tumors reveals potential therapeutic targets (top 9 are shown) **(a)**. CD47 is highly expressed on all PanNET cells by flow cytometry **(b)** and immuno-fluorescence **(c)**. CD47 is co-expressed with MET **(d)**. CD47 expression is enhanced in the CD90^{hi} cells (TICs) compared to CD90^{neg} cells **(e)**. Kaplan-Meier analysis of tissue microarray staining show that increased CD47 expression is associated with decreased survival compared to decreased CD47 expression **(f)**. High-throughput phagocytosis assays were used to validate potential therapeutic targets **(g-h)**. In-vitro phagocytosis of PanNET cells by macrophages is enhanced with anti-CD47 and anti-CD99 therapies as well as cetuximab **(c-e)**.

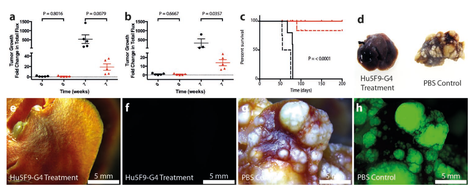

Figure 7. Anti-CD47 therapy initiated 2 weeks **(a)** and 3 weeks **(b)** after orthotopic APL1 xenograft engraftment in NSG mice inhibits tumor growth compared to controls. Anti-CD47 therapy prolongs survival in both 2- and 3-week engraftment cohorts compared to controls **(c)**. Anti-CD47 therapy prevents hepatic metastases **(d-h)** in vivo compared to untreated controls.

Results

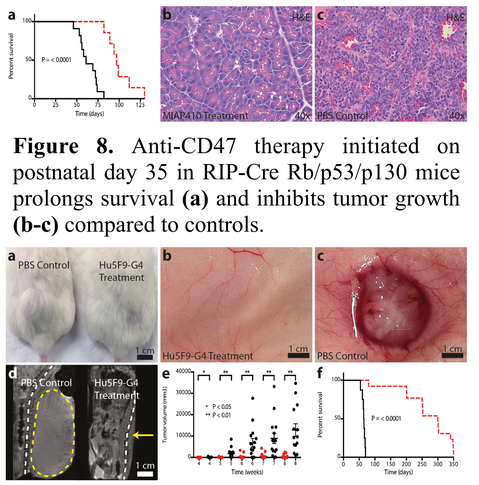

Figure 8. Anti-CD47 therapy initiated on postnatal day 35 in RIP-Cre Rb/p53/p130 mice prolongs survival **(a)** and inhibits tumor growth **(b-c)** compared to controls.

Figure 9. Anti-CD47 therapy initiated 2 weeks after primary patient heterotopic xenograft engraftment in NSG mice inhibits tumor growth **(a-e)** prolongs survival **(f)** compared to controls.

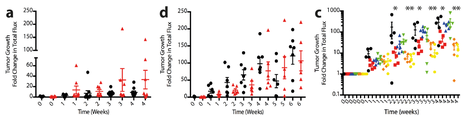

Figure 10. Anti-CD99 **(a)** and anti-CD59 **(b)** therapies do not inhibit tumor growth in vivo compared to controls. Anti-EGFR therapies alone do not inhibit tumor growth in vivo **(c)**. Combination of anti-CD47 and anti-EGFR therapies inhibits tumor growth to a greater degree than either therapy alone in vivo **(c)**.

Conclusions

- MET activation is critical for tumor growth in mouse xenograft models
- CD90 characterizes TICs in PanNETs
- Proteomic profiling reveals potential therapeutic targets that were screened with in vitro phagocytosis assays
- Anti-CD47 therapy inhibits tumor growth, prolongs survival, and prevents metastases in vivo
- Anti-CD47 therapy may synergize with other immunotherapies